HHS Public Access

Author manuscript

J Biomed Mater Res A. Author manuscript; available in PMC 2018 April 01.

Published in final edited form as:

J Biomed Mater Res A. 2017 April ; 105(4): 1230–1236. doi:10.1002/jbm.a.35974.

SPHEROID MODEL FOR FUNCTIONAL OSTEOGENIC EVALUATION OF HUMAN ADIPOSE DERIVED STEM CELLS

Bhuvaneswari Gurumurthy[#], **Patrick C. Bierdeman**[#], and **Amol V. Janorkar**[*]

Department of Biomedical Materials Science, School of Dentistry, University of Mississippi Medical Center, Jackson, Mississippi, 39216

Abstract

3D culture systems have the ability to mimic the natural microenvironment by allowing better cell-cell interactions. We have prepared an *in vitro* 3D osteogenic cell culture model using human adipose derived stem cells (hASCs) cultured atop recombinant elastin-like polypeptide (ELP) conjugated to a charged polyelectrolyte, polyethyleneimine (PEI). We demonstrate that hASCs cultured atop the ELP-PEI coated tissue culture polystyrene (TCPS) formed 3D spheroids and exhibited superior differentiation toward osteogenic lineage compared to the traditional two dimensional (2D) monolayer formed atop uncoated TCPS. Live/dead viability assay confirmed >90% live cells at the end of the 3-week culture period. Over the same culture period, higher protein content was observed in 2D monolayer than 3D spheroids, as the 2D environment allowed continued proliferation, while 3D spheroids underwent contact-inhibited growth arrest. The normalized alkaline phosphatase (ALP) activity, which is an indicator for early osteogenic differentiation was higher for 3D spheroids. The normalized osteocalcin (OCN) production, which is an indicator for osteogenic maturation was also higher for 3D spheroids while 2D monolayer had no noticeable OCN production. On day 22, increased Alizarin red uptake by 3D spheroids showed greater mineralization activity than 2D monolayer. Taken together, these results indicate a superior osteogenic differentiation of hASCs in 3D spheroid culture atop ELP-PEI coated TCPS surfaces than the 2D monolayer formed on uncoated TCPS surfaces. Such enhanced osteogenesis in 3D spheroid stem cell culture may serve as an alternative to 2D culture by providing a better microenvironment for the enhanced cellular functions and interactions in bone tissue engineering.

Keywords

Elastin-like polypeptide; Bone tissue engineering; 3D spheroids; in vitro 3D model; Osteogenesis

1. INTRODUCTION

The success of tissue engineering largely depends on mimicking the 3D complex microenvironment. The *in vitro* 3D cell culture microenvironments can be broadly classified as cells cultured in biomimetic scaffolds and cells cultured in aggregates. Scaffolds allow culture by encapsulating cells in a 3D arrangement and rely on extensive cell-matrix

[*]Corresponding author: Telephone: (601) 984-6170; Fax: (601) 984-6087; ajanorkar@umc.edu.
[#]Equal contribution

interactions, but often allow inadequate cell-cell interactions and, the difficulty in controlling the scaffold mechanical and physical properties limits cell culture performance [1,2]. The cellular aggregates, a.k.a. 3D spheroids, can be prepared in a “scaffold-free” culture and are formed when the cells do not preferentially adhere to any substrate and instead attach to themselves through junctional complexes [3]. Spheroids have been shown to create *in vivo* like functionality by having anatomical and physiological similarities with the native tissues such as cardiomyocyte spheroids beating in a heart-like rhythm, hepatocyte spheroids having liver-like performance, as well as human endothelial cells vascularizing microtissues [4–6]. Spheroids recapitulate complex cell-cell and cell-ECM interactions to effectively communicate mechanical and biochemical signals that can influence cell shape, proliferation, differentiation, and gene expression [7]. As such, molecular gradients of soluble components added in the cell culture medium (e.g., nutrients and growth factors) as well as the metabolites produced by the cells are established in 3D spheroids due to the formation of diffusion barrier leading to differential rates of production and consumption of these factors [8,9].

Scaffold-free 3D spheroid cultures have been produced previously by both static (hanging drop and micro-patterned surfaces) and dynamic (spinner flask and rotating vessel wall) cultures, but both techniques have problems associated with them. Some of the problems include difficulty in visualizing spheroids, damage to cells due to shear forces, and difficulty in controlling spheroid sizes [10]. Scaffold-free 3D spheroids can also be created using positively-charged surface coatings [11], however the spheroids formed on the non-adherent surfaces are more prone to dislodgement, resulting in reduced tissue specific functions. Also, the positively charged polymers may be cytotoxic and can only be used in low concentrations, which may lead to a surface with uneven coating. To overcome these problems, we have devised a 3D spheroid culture technique using a coating of genetically engineered polymer elastin-like polypeptide (ELP) conjugated with a polyelectrolyte polyethyleneimine (PEI). Given that ECM is composed of elastin and the ELP is a recombinant form of mammalian elastin, ELP can provide a recognizable environment for the cell attachment. The ELP-PEI forms a positively charged coating on the TCPS surface with the PEI component being responsible for the formation of spheroids, while the ELP component facilitating the surface attachment of the formed spheroids. The ELP and PEI conjugation reaction conditions and the concentration of ELP-PEI surface coating for spheroid formation have already been optimized in such a way as to not affect the viability of the cells [12]. Using this substrate, we have successfully prepared 3D spheroids of primary rat hepatocytes, 3T3-L1 adipocytes, and H35 rat hepatoma cells [12–14]. We have demonstrated a superior differentiation in the 3D spheroids formed from these cells compared to the 2D monolayer culture [12–14].

The 3D spheroid model can be used for tissue regeneration using adult mesenchymal stem cells (MSCs) that have multi-lineage potential. With increased differentiation capability and potential of progenitor cells, stem cells like salivary gland-derived progenitor cells differentiate into hepatocytic and pancreatic lineages only in 3D spheroid environment [15]. Additionally, neuronal differentiation of embryonic stem cells [16] and odonto/osteo differentiation of dental pulpal stem cells [17] have higher efficacy in spheroids. 3D spheroid culture model for culture and differentiation of MSCs into osteogenic lineage will

be of significance in bone regeneration, as the bone tissue specific functionality of the osteogenic cells will be raised due to the intercellular interactions. Strong evidence has been shown to prove that 3D microenvironment is needed for osteogenic differentiation [18–20]. Kale et al. have shown that 3D spheroids cause early up-regulation of several bone related markers like alkaline phosphatase (ALP), collagen type I, and osteonectin with concomitant bone formation in human osteogenic cells [21]. Human adipose derived stem cells (hASCs) are analogous to the bone marrow MSCs (BMSCs). hASCs have been widely used in regenerating skin, bone, fat, cartilage and cardiovascular tissues [22]. hASCs are used as an alternative to BMSCs due to their easy procurement, high harvest yield, and rapid *in vitro* expansion [23]. In this study, we studied the *in vitro* osteogenic activity of hASCs, by culturing them as spheroids in TCPS plates coated with ELP-PEI. We hypothesized that the spheroids formed from hASCs will have long term stability and greater differentiation towards osteogenic lineage when compared to the traditional 2D monolayer. To this end, over a 3-week culture period, we performed head-to-head comparisons between the 2D monolayer and 3D spheroid cultures with respect to protein content, ALP activity, osteocalcin (OCN) production, mineralization by Alizarin red staining.

2. MATERIALS AND METHODS

2.1 Expression, purification and chemical modification of ELP

Escherichia coli bacteria with synthetic gene for $(VPGVG)_{40}$ (V = valine, P = proline, G = glycine), were multiplied in a suspension culture of nutrient broth and purified by inverse phase transition cycling as described elsewhere [24]. The purified ELP was dialyzed against deionized water and then lyophilized. ELP was chemically conjugated to PEI (MW = 800 Da, Sigma, St. Louis, MO, USA) using activation of ELP with N-hydroxysuccinimide and 1-ethyl-3-(3-dimethyl aminopropyl) carbodiimide hydrochloride (Sigma, St. Louis, MO) as previously described [12].

2.2 ELP-PEI Coating

ELP-PEI coating was formed according to our previous studies [12, 14]. ELP-PEI conjugate was adsorbed to 24-well TCPS plate (Corning Costar, Corning, NY, USA) by placing 200 μL of 5 mol% ELP-PEI solution and incubating at 37 °C for 48 h in a dry incubator.

2.3 hASC culture

hASCs were obtained according to our Institutional Review Board (IRB)-approved protocol (# 2012–0004) from lipoaspirates of an unidentified female patient who underwent elective liposuction procedure. hASCs were maintained and expanded in Dulbecco's modified eagle's medium (DMEM) (Hyclone labs, South Logan, UT, USA) supplemented with 10% calf serum, 2 mM L-glutamine, 100 U/mL penicillin and 100 μg/mL streptomycin, and 2 mM sodium pyruvate (Invitrogen, Carlsbad, CA, USA) with pH adjusted to 7.4. Cells were harvested at 80% confluence by trypsinization. 50,000 cells were seeded onto uncoated and ELP-PEI coated TCPS surfaces of each well of a 24-well culture plate. The hASCs were cultured for 3 days either to generate 3D spheroids atop ELP-PEI coated surfaces or to reach confluence as a 2D monolayer atop uncoated TCPS surfaces. Subsequently, the cells were supplemented with osteogenic differentiation medium containing DMEM, 50 mM L-

ascorbic acid, 10 nM dexamethasone, 10 mM β-glycerophosphate, 10% fetal bovine serum, and 100 U/mL penicillin and 100 μg/mL streptomycin for 3 weeks. Fresh media was fed every 48 hours. The experiment timeline is shown in Figure 1.

2.4 Imaging

IX-81 epifluorescence microscope (Olympus, Center Valley, PA, USA) was used to image the 2D monolayer and 3D spheroids under bright field on days 8 and 22. Bright field, FITC and TRITC filters were used for cell viability assessment (n = 3) using live/dead assay (Invitrogen) on day 22. The cells were treated with live/dead reagents and SlideBook software (Olympus, Center Valley, PA, USA) was used for image analysis.

2.5 Biochemical Analyses

All the assays were performed as per the manufacturers' instructions. To quantify the total protein content, ALP activity, and osteocalcin production, 2D monolayer and 3D spheroids were collected by trypsinization and mechanical squirting action, respectively. Cells were pelleted by centrifugation at 3,500 rpm for 5 min, washed with PBS, and spun again at 3,500 rpm for 5 min. The pellet was resuspended in PBS and sonicated for 30 s at 10% amplitude using a Branson Digital Sonifier 450 (Branson, Danbury, CT, USA). Total protein present in the cells collected on days 1, 8, 15 and 22 (n = 3) was measured by BCA total protein assay (Thermo Scientific, Rockford, IL, USA) and quantified by comparison against standard curves constructed from manufacturer's standards. The protein level was measured with a 540 nm filter on ELX-800 absorbance plate reader (Biotek, Winooski, VT). Total protein data was used to normalize the data collected from other assays namely, ALP activity assay (n = 3), osteocalcin assay (n = 3), and Alizarin red staining (n = 3). Quantichrom ALP assay (BioAssay Systems, Hayward, CA) was used for colorimetric determination of ALP activity of cells collected on days 8, 15 and 22. The absorbance was measured at 0 and 4 min at 405 nm on ELX-800 absorbance plate reader, and ALP activity was calculated. Osteocalcin assay (OCN) (Invitrogen, Carlsbad, CA) was used to perform an ELISA specific for human osteocalcin. The absorbance was measured at 450 nm on ELX-800 absorbance plate reader and OCN production was calculated. Next, osteogenesis quantitation kit (EMD Millipore, Billerica, MA) was used to determine the mineralization activity on day 22. The differentiated cells with bright red stained mineralized deposits were seen using EVOS™ FL cell imaging system (Life Technologies, Carlsbad, CA). Quantitative determination was done by further incubating the cells in 10% acetic acid with shaking for 30 min followed by vigorous vortexing for 30 s, and heating at 85 °C for 10 min. The extract was centrifuged at 22,000×g for 15 min, neutralized with 150 μL of 10% ammonium hydroxide and absorbance was measured at 405 nm on ELX-800 absorbance plate reader.

2.6 Statistical Analysis

All experiments were performed in triplicate. Results were reported as mean ± 95% confidence intervals. Statistical analysis was done using ANOVA. Values with $p \leq 0.05$ were deemed statistically significant.

3. RESULTS

The 2D *in vitro* culture model was created by achieving a confluent monolayer of hASCs seeded on uncoated TCPS surface, and supplementing them with osteogenic differentiation media (Figure 2a,b). The positively charged ELP-PEI coated TCPS surface led to the creation of 3D spheroids of hASCs, which received the same osteogenic differentiation media and formed 3D *in vitro* culture model (Figure 2c,d). The uncoated TCPS surface had the hASCs proliferate and spread out to confluence on the entire surface displaying traditional 2D monolayer features. But, the ELP-PEI coated TCPS surface induced the hASCs to form aggregates in the first 24 hours and spheroids by 72 hours. After the 3 days, when cells were fed differentiation media, 2D and 3D cultures reacted by showing osteogenic differentiation. On visual inspection microscopically, the spheroid sizes continued to increase over the 3-week culture period (Figure 2a–d). To assess the cell viability, live/dead assay was performed on day 22 (Figure 2e–h). The red fluorescence indicated dead cells while the green fluorescence indicated the presence of live cells. Though some dead cells were seen in the 3D spheroids (Figure 2h), the percentage of live cells was more than 90%, similar to that in the 2D monolayer indicating that the cells did not experience any significant cytotoxicity due to exposure to ELP-PEI or due to the 3D spheroid configuration (Figure 2i).

Over the 3-week culture period, the cells were harvested for determining the total protein content, ALP activity, OCN content, and Alizarin red stain uptake. As shown in Figure 3, the total protein content of the cells cultured as 3D spheroids was significantly lower than those cultured as 2D monolayer on all days ($p < 0.05$ on same day). The cells cultured as 2D monolayer had increasing total protein content from day 1 (127.5 ± 23.6 μg) to day 22 (407.5 ± 56.7 μg). In contrast, the protein content of cells cultured as 3D spheroids only showed an increase from day 1 (22.4 ± 6.2 μg) to day 8 (47.7 ± 9.2 μg) after which it plateaued until day 22.

Figure 4, shows the ALP activity of hASCs normalized to total protein content, which serves as an early marker for osteogenic differentiation. The normalized ALP activity on day 8 for 3D spheroids was 33.6 ± 5.2 nM/min/μg protein, while the same for 2D monolayer was 12.8 ± 5.1 nM/min/μg protein. Similar trend of the significantly higher normalized ALP activity for the 3D spheroids compared to the 2D monolayer was observed on all days, and this difference was statistically significant on days 8 and 22 ($p < 0.05$ on same day).

To assess the osteogenic maturation response, hASCs cultured as 2D monolayer and 3D spheroids were analyzed for osteocalcin production. The normalized osteocalcin production in 3D spheroids was between 0.6 and 1.5 pg/μg protein on days 8, 15, and 22, with the highest osteocalcin production of 1.56 ± 0.44 pg/μg protein on day 22 for 3D spheroids (Figure 5). The 2D monolayer showed minimal osteocalcin production (Figure 5), which was significantly lower than that for the 3D spheroids on all days ($p < 0.05$).

Visualization of Alizarin red staining on day 22 showed negligible amount of mineralized deposits in 2D monolayer, while the 3D spheroids showed bright red staining on the spheroids (Figure 6a,b). Quantification of mineralization using the concentration of

extracted alizarin red stain normalized to total protein, also showed that 3D spheroids had greater mineralization (0.19 ± 0.15 nM/μg protein) compared to negligible mineralization (0.000 ± 0.003 nM/μg protein) in the 2D monolayer ($p = 0.06$), as seen in Figure 6c.

4. DISCUSSION

Conventional 2D culture techniques fail to reproduce a physiologically-relevant 3D environment and yield poor cell differentiation of mesenchymal cells [25, 26]. The 3D spheroids are increasingly gaining popularity in tissue engineering due to extensive cell-cell interactions possible in this configuration that may result in a superior cellular differentiation [27]. Multiple culture methods like pellet culture, micromass culture, culture on micro-patterned surfaces, suspension culture, hanging drop culture, and rotating wall vessel are used to generate 3D spheroids [8, 28]. In contrast to studies reporting the formation of spheroids by these complex methods that may be associated with problems in visualizing, maintenance of stability and controlling the damage to spheroids [10], we have developed conditions whereby hASCs undergo osteogenic differentiation without requiring complex equipment or cumbersome techniques. Our system has the unique advantage of forming stable spheroids by their attachment to a biocompatible material such as ELP, and also their formation using a low concentration of the polyelectrolyte polymer, that decreased the cytotoxic effect. In our previous studies, we have demonstrated that 3D spheroid formation could be induced over positively charged ELP-PEI coated surfaces [13,14]. By using this method now, we have cultured spheroids of hASCs. The hASCs spheroids formed over a period of 72 h and maintained the cell-cell junctions by self-assembly just like the H35 rat hepatoma cells, 3T3-L1 pre-adipocytes, and primary rat hepatocytes [12–14]. Unlike the previous experiments done with cells that were committed to a specific-lineage (3T3-L1 pre-adipocytes), were terminally differentiated (primary rat hepatocytes), or were an immortal cell line (H35 rat hepatoma cells), the results from this study are unique as hASCs are multipotent stem cells and have a demonstrated ability to differentiate along a variety of lineages depending on the microenvironmental cues. It should also be noted that previous work has largely focused on generating 3D spheroids of animal cells, while this work has generated 3D spheroids of human origin.

In the live/dead assay (Figure 2) our results showed equal viability of cells in uncoated and ELP-PEI coated TCPS surfaces which demonstrated that an otherwise cytotoxic PEI gained biocompatibility when conjugated with ELP. The cell viability on day 22 is similar to the monolayer, confirming that ELP-PEI system is a viable alternative to 2D cell culture. The live/dead staining of our spheroids had a similar appearance to that of the commercial MSCs that underwent osteogenesis and imaged on day 26 by Wang et al. [28]. We observed that the dead cells concentrated toward the central region of the spheroids (Figure 2h) which may be due to limitation on the diffusion of oxygen, nutrient supply, and growth factors, as noted by Crucio et al. in mouse hepatocytes and Hu et al. in multicellular tumor cells [29,30]. The total protein content in the 3D spheroids were much lower than the 2D monolayer as shown in Figure 3 and early plateauing demonstrates the formation of stable spheroids as well as their restricted proliferation. This outcome is similar to our previous work with H35 rat hepatoma cells and 3T3-L1 pre-adipocytes [13,14]. The spheroids are attached to ELP portion of the ELP-PEI coating by means of surface-tethering, which in turn restricts the loss

of spheroids with time, leading to plateaued protein content. The cells in 3D culture interact with their adjacent neighbors resulting in a contact-inhibited, reduced proliferation. Also, unlike in the 2D monolayer, the spheroids do not have a firm attachment to the TCPS surface. This may further reduce their expansion potential, as observed by Schmal et al. in spheroids formed with MSCs of umbilical origin [31].

Considering the reciprocal relationship between proliferation and differentiation, we then expected to observe a superior osteogenic differentiation in our 3D spheroid culture. To study the osteogenic differentiation and maturation capacity of hASCs cultured on ELP-PEI coated and uncoated TCPS surfaces, we selected two of the well-researched early and late markers of differentiation, namely, ALP activity and OCN production. In addition, as a marker for osteogenic maturation, the presence of calcified matrix from cells in both monolayer and spheroids was visualized and quantified by Alizarin red staining. Our study has shown that reorganization of hASCs into spheroids over ELP-PEI coated surfaces did not disrupt their ability to undergo osteogenesis when stimulated with specific differentiation medium. In fact, the 3D spheroids had relatively greater amounts of osteogenic activity compared to the 2D monolayer as measured by ALP activity (Figure 4), OCN production (Figure 5), and Alizarin red levels (Figure 6). Remarkably, the OCN production and Alizarin red staining was insignificant in 2D monolayer indicating a negligible osteogenic capacity. We posit that the enhanced osteogenic differentiation of spheroids compared to monolayer can be because of: difference in tension between hASCs adhering to the TCPS plate in monolayer versus the natural ECM in spheroids, as matrix elasticity can affect cell differentiation [32], accelerated mineralization due to enhanced secretion of bone specific ECM [33], superior cell-cell contacts resulting in high cell density in spheroids [34], and initiation of differentiation as cells contact with one another and with ECM [33]. Overall, our results agree well with other studies that have demonstrated osteogenic differentiation of stem cells. For instance, the ALP activity of our 3D spheroid hASC culture was higher on day 15 similar to the BMSCs cultured as microaggregates in Aggrewell™ [25]. The higher Alizarin red staining observed in our 3D spheroid hASC culture was similar to that observed in commercial human MSCs cultured on micro-patterned surfaces by Wang et al. [28]. Similar results were also observed by Yamaguchi at al., in their study with rat BMSCs [35].

5. CONCLUSION

This work describes a 3D spheroid model of hASCs formed using ELP-PEI coating of TCPS surfaces to study the osteogenic differentiation, maturation and mineralization. Taken together, we have used the ELP-PEI coating method for *in vitro* 3D spheroid culture and shown that hASCs cultured in this way have improved differentiation properties compared to the 2D monolayer culture. Future studies involving our 3D spheroid model would investigate the applications in bone tissue engineering by using 3D spheroids in composite guided bone regeneration scaffolds.

Acknowledgments

This study was sponsored by the National Institute of Dental and Craniofacial Research of the National Institutes of Health under Award Number R03DE024257. The content is solely the responsibility of the authors and does not necessarily represent the official views of the National Institutes of Health. PCB participated in the Undergraduate

and Professional Student Training in Advanced Research Techniques (UPSTART) Program. This work made use of instruments in the Department of Biomedical Materials Science User Facility. We thank Dr. Peter Arnold for the procurement of the donated whole adipose tissue. The use of the human cells in this research was approved by the University of Mississippi Medical Center Institutional Review Board.

References

1. Eleanor K, Przyborski S. Advances in 3D culture technologies enabling tissue-like structures to be created in vitro. J Anat. 2015; 227:746–56. [PubMed: 25411113]
2. Sun J, Tan H. Alginate-based biomaterials for regenerative medicine applications. Materials. 2013; 6:1285–1309.
3. Mueller-Klieser W. Three-dimensional cell cultures: from molecular mechanisms to clinical applications. Am J Physiol. 1997; 273:C1109–23. [PubMed: 9357753]
4. Fukuda J, Nakazawa K. Orderly arrangement of hepatocyte spheroids on a microfabricated chip. Tissue Eng. 2005; 11:1254–62. [PubMed: 16144461]
5. Desroches BR, Zhang P, Choi BR, King ME, Maldonado AE, Li W, Rago A, Liu G, Nath N, Hartmann KM, Yang B, Koren G, Morgan JR, Mende U. Functional scaffold-free 3-D cardiac microtissues: a novel model for the investigation of heart cells. Am J Physiol Heart Circ Physiol. 2012; 302:H2031–42. [PubMed: 22427522]
6. Kunz-Schughart LA, Schroeder JA, Wondrak M, van Rey F, Lehle K, Hofstaedter F, Wheatley DN. Potential of fibroblasts to regulate the formation of three-dimensional vessel-like structures from endothelial cells in vitro. Am J Physiol Cell Physiol. 2006; 290:C1385–98. [PubMed: 16601149]
7. Pampaloni F, Reynaud EG, Stelzer EH. The third dimension bridges the gap between cell culture and live tissue. Nat Rev Mol Cell Biol. 2007; 8:839–45. [PubMed: 17684528]
8. Achilli TM, Meyer J, Morgan JR. Advances in the formation, use and understanding of multi-cellular spheroids. Expert Opin Biol Ther. 2012; 12:1347–60. [PubMed: 22784238]
9. Griffith LG, Swartz MA. Capturing complex 3D tissue physiology in vitro. Nat Rev Mol Cell Biol. 2006; 7:211–24. [PubMed: 16496023]
10. Lin RZ, Chang HY. Recent advances in three-dimensional multicellular spheroid culture for biomedical research. Biotechnol J. 2008; 3:1172–84. [PubMed: 18566957]
11. Koide N, Sakaguchi K, Koide Y, Asano K, Kawaguchi M, Matsushima H, Takenami T, Shinji T, Mori M, Tsuji T. Formation of multicellular spheroids composed of adult rat hepatocytes in dishes with positively charged surfaces and under other nonadherent environments. Exp Cell Res. 1990; 186:227–35. [PubMed: 2298241]
12. Turner PA, Weeks CA, McMurphy AJ, Janorkar AV. Spheroid organization kinetics of H35 rat hepatoma model cell system on elastin-like polypeptide-polyethyleneimine copolymer substrates. J Biomed Mater Res A. 2014; 102:852–61. [PubMed: 23564487]
13. Janorkar AV, Rajagopalan P, Yarmush ML, Megeed Z. The use of elastin-like polypeptide-polyelectrolyte complexes to control hepatocyte morphology and function in vitro. Biomaterials. 2008; 29:625–32. [PubMed: 18006054]
14. Turner PA, Harris LM, Purser CA, Baker RC, Janorkar AV. A surface-tethered spheroid model for functional evaluation of 3T3-L1 adipocytes. Biotechnol Bioeng. 2014; 111:174–83. [PubMed: 24038000]
15. Okumura K, Nakamura K, Hisatomi Y, Nagano K, Tanaka Y, Terada K, Sugiyama T, Umeyama K, Matsumoto K, Yamamoto T, Endo F. Salivary gland progenitor cells induced by duct ligation differentiate into hepatic and pancreatic lineages. Hepatology. 2003; 38:104–13. [PubMed: 12829992]
16. Watanabe K, Kamiya D, Nishiyama A, Katayama T, Nozaki S, Kawasaki H, Watanabe Y, Mizuseki K, Sasai Y. Directed differentiation of telencephalic precursors from embryonic stem cells. Nat Neurosci. 2005; 8:288–96. [PubMed: 15696161]
17. Xiao L, Tsutsui T. Characterization of human dental pulp cells-derived spheroids in serum-free medium: stem cells in the core. J Cell Biochem. 2013; 114:2624–36. [PubMed: 23794488]
18. Lammers L, Naujoks C, Berr K, Depprich R, Kubler N, Meyer U, Langenbach F, Luttenberg B, Kogler G, Wiesmann HP, Handschel J. Impact of DAG stimulation on mineral synthesis, mineral

structure and osteogenic differentiation of human cord blood stem cells. Stem Cell Res. 2012; 8:193–205. [PubMed: 22265739]

19. Langenbach F, Naujoks C, Kersten-Thiele PV, Berr K, Depprich RA, Kubler NR, Kogler G, Handschel J. Osteogenic differentiation influences stem cell migration out of scaffold-free microspheres. Tissue Eng Part A. 2010; 16:759–66. [PubMed: 19772456]
20. Langenbach F, Berr K, Naujoks C, Hassel A, Hentschel M, Depprich R, Kubler NR, Meyer U, Wiesmann HP, Kogler G, Handschel J. Generation and differentiation of microtissues from multipotent precursor cells for use in tissue engineering. Nat Protoc. 2011; 6:1726–35. [PubMed: 22011655]
21. Kale S, Biermann S, Edwards C, Tarnowski C, Morris M, Long MW. Three-dimensional cellular development is essential for ex vivo formation of human bone. Nat Biotechnol. 2000; 18:954–8. [PubMed: 10973215]
22. Takiyama N, Mizuno T, Iwai R, Uechi M, Nakayama Y. In-body tissue-engineered collagenous connective tissue membranes (BIOSHEETs) for potential corneal stromal substitution. J Tissue Eng Regen Med. 2013
23. Strem BM, Hicok KC, Zhu M, Wulur I, Alfonso Z, Schreiber RE, Fraser JK, Hedrick MH. Multipotential differentiation of adipose tissue-derived stem cells. Keio J Med. 2005; 54:132–41. [PubMed: 16237275]
24. Amruthwar SS, Janorkar AV. In vitro evaluation of elastin-like polypeptide-collagen composite scaffold for bone tissue engineering. Dent Mater. 2013; 29:211–20. [PubMed: 23127995]
25. Kabiri M, Kul B, Lott WB, Futrega K, Ghanavi P, Upton Z, Doran MR. 3D mesenchymal stem/stromal cell osteogenesis and autocrine signalling. Biochem Biophys Res Commun. 2012; 419:142–7. [PubMed: 22266317]
26. Gruber HE, Hanley EN Jr. Human disc cells in monolayer vs 3D culture: cell shape, division and matrix formation. BMC Musculoskelet Disord. 2000; 1:1. [PubMed: 11231882]
27. Cesarz Z, Tamama K. Spheroid Culture of Mesenchymal Stem Cells. Stem Cells Int. 2016:9176357. [PubMed: 26649054]
28. Wang W, Itaka K, Ohba S, Nishiyama N, Chung UI, Yamasaki Y, Kataoka K. 3D spheroid culture system on micropatterned substrates for improved differentiation efficiency of multipotent mesenchymal stem cells. Biomaterials. 2009; 30:2705–15. [PubMed: 19215979]
29. Curcio E, Salerno S, Barbieri G, De Bartolo L, Drioli E, Bader A. Mass transfer and metabolic reactions in hepatocyte spheroids cultured in rotating wall gas-permeable membrane system. Biomaterials. 2007; 28:5487–97. [PubMed: 17881050]
30. Hu G, Li D. Three-dimensional modeling of transport of nutrients for multicellular tumor spheroid culture in a microchannel. Biomed Microdevices. 2007; 9:315–23. [PubMed: 17203380]
31. Schmal O, Seifert J, Schaffer TE, Walter CB, Aicher WK, Klein G. Hematopoietic Stem and Progenitor Cell Expansion in Contact with Mesenchymal Stromal Cells in a Hanging Drop Model Uncovers Disadvantages of 3D Culture. Stem Cells Int. 2016:4148093. [PubMed: 26839560]
32. Engler AJ, Sen S, Sweeney HL, Discher DE. Matrix elasticity directs stem cell lineage specification. Cell. 2006; 126:677–89. [PubMed: 16923388]
33. Langenbach F, Naujoks C, Smeets R, Berr K, Depprich R, Kubler N, Handschel J. Scaffold-free microtissues: differences from monolayer cultures and their potential in bone tissue engineering. Clin Oral Investig. 2013; 17:9–17.
34. Bitar M, Brown RA, Salih V, Kidane AG, Knowles JC, Nazhat SN. Effect of cell density on osteoblastic differentiation and matrix degradation of biomimetic dense collagen scaffolds. Biomacromolecules. 2008; 9:129–35. [PubMed: 18095652]
35. Yamaguchi Y, Ohno J, Sato A, Kido H, Fukushima T. Mesenchymal stem cell spheroids exhibit enhanced in-vitro and in-vivo osteoregenerative potential. BMC Biotechnol. 2014; 14:105. [PubMed: 25479895]

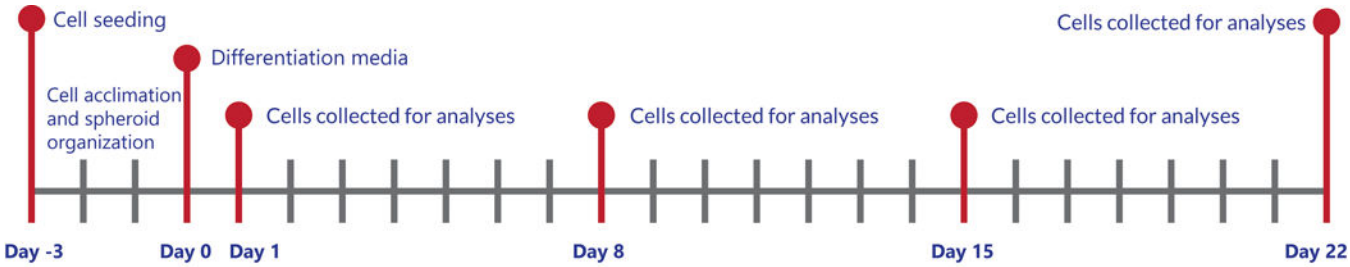

Figure 1.
Timeline of experiment.

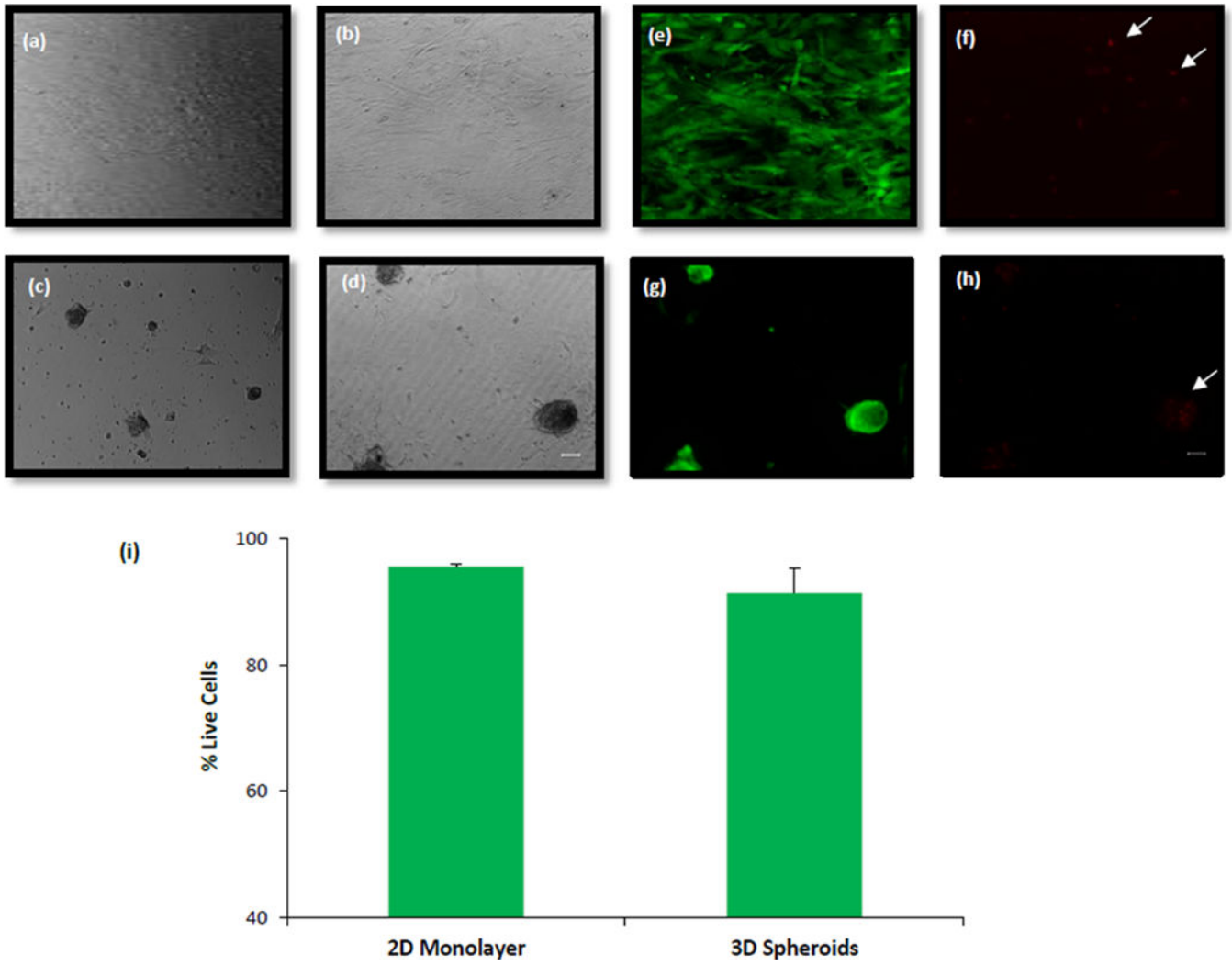

Figure 2.

Bright field images of hASCs (a, b) 2D monolayer and (c, d) 3D spheroids on days 8 (a, c) and 22 (b, d). Live/Dead images (e, f, g, h) and quantification (i) of hASC viability on day 22 in 2D and 3D cells. Scale bar = 50 μm.

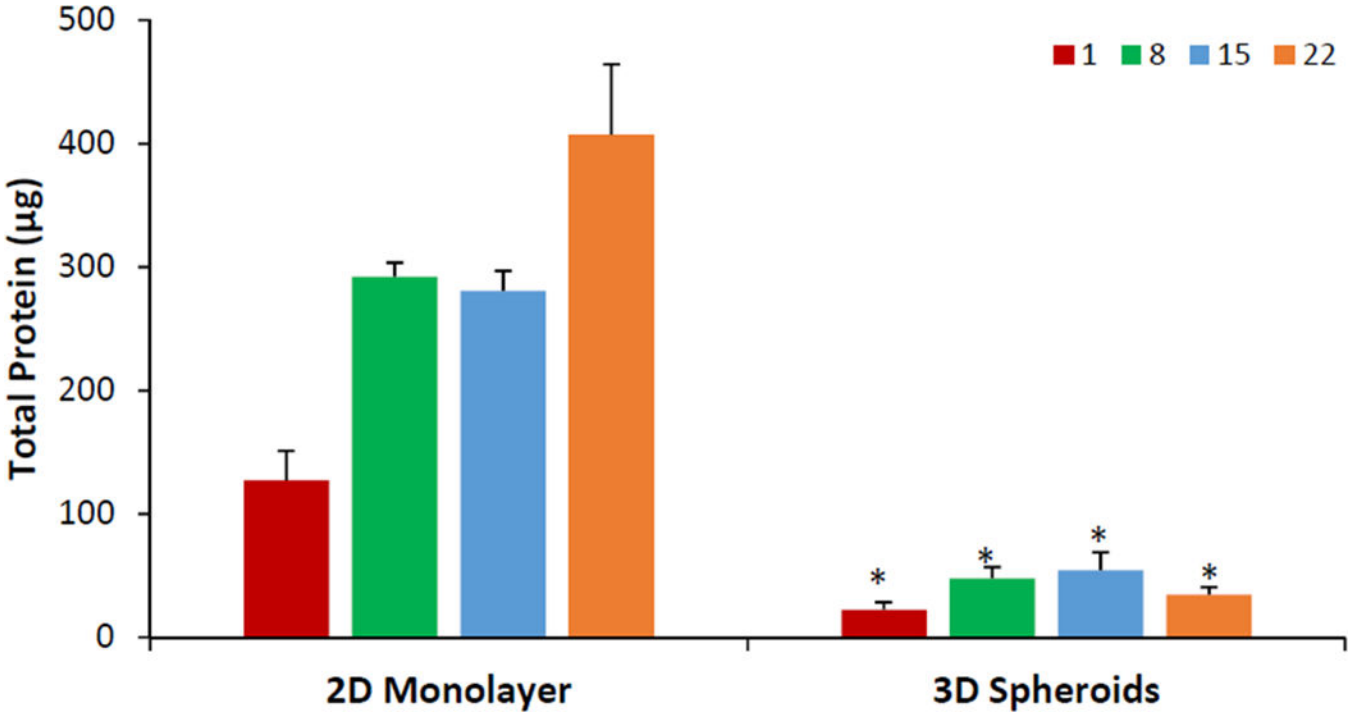

Figure 3.

Total protein content of hASCs cultured as 2D monolayer and 3D spheroids. Red bars = day 1; green bars = day 8; blue bars = day 15, orange bars = day 22. Error bars represent 95% confidence intervals. *$p \leq 0.05$ against 2D on the same day.

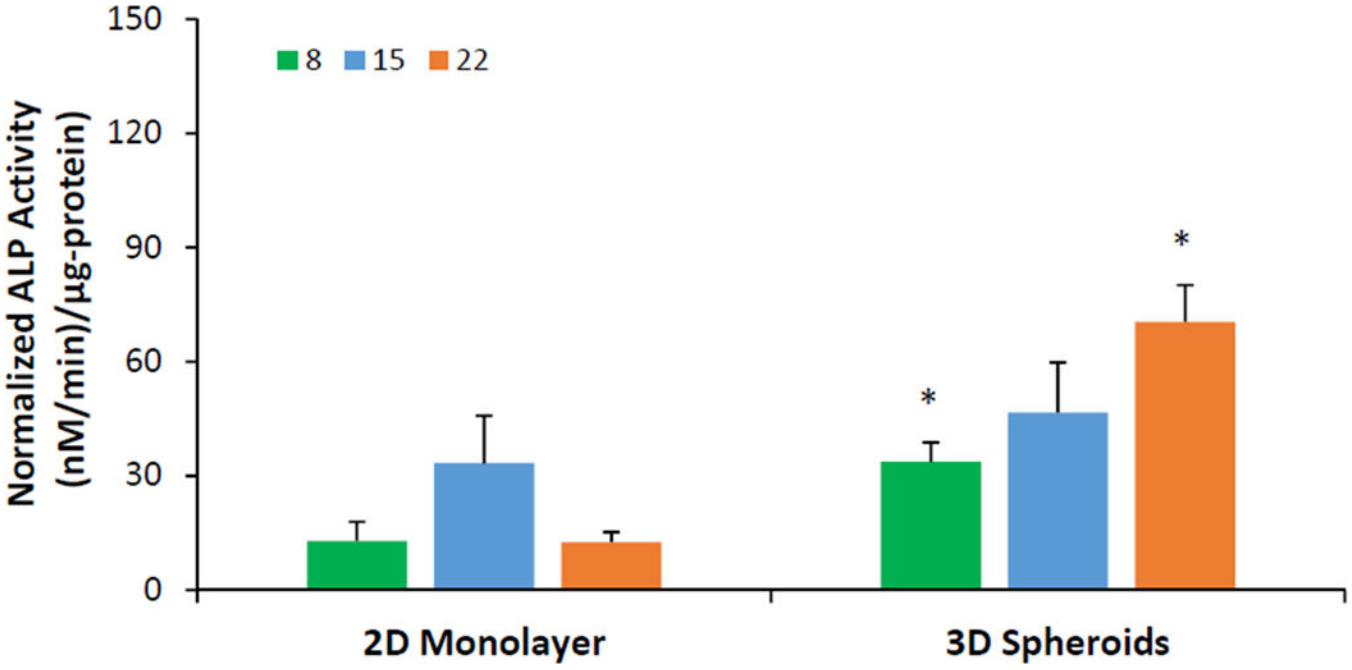

Figure 4.

ALP activity normalized to total protein of hASCs cultured as 2D monolayer and 3D spheroids. Green bars = day 8; blue bars = day 15, orange bars = day 22. Error bars represent 95% confidence intervals. *$p \leq 0.05$ against 2D on the same day.

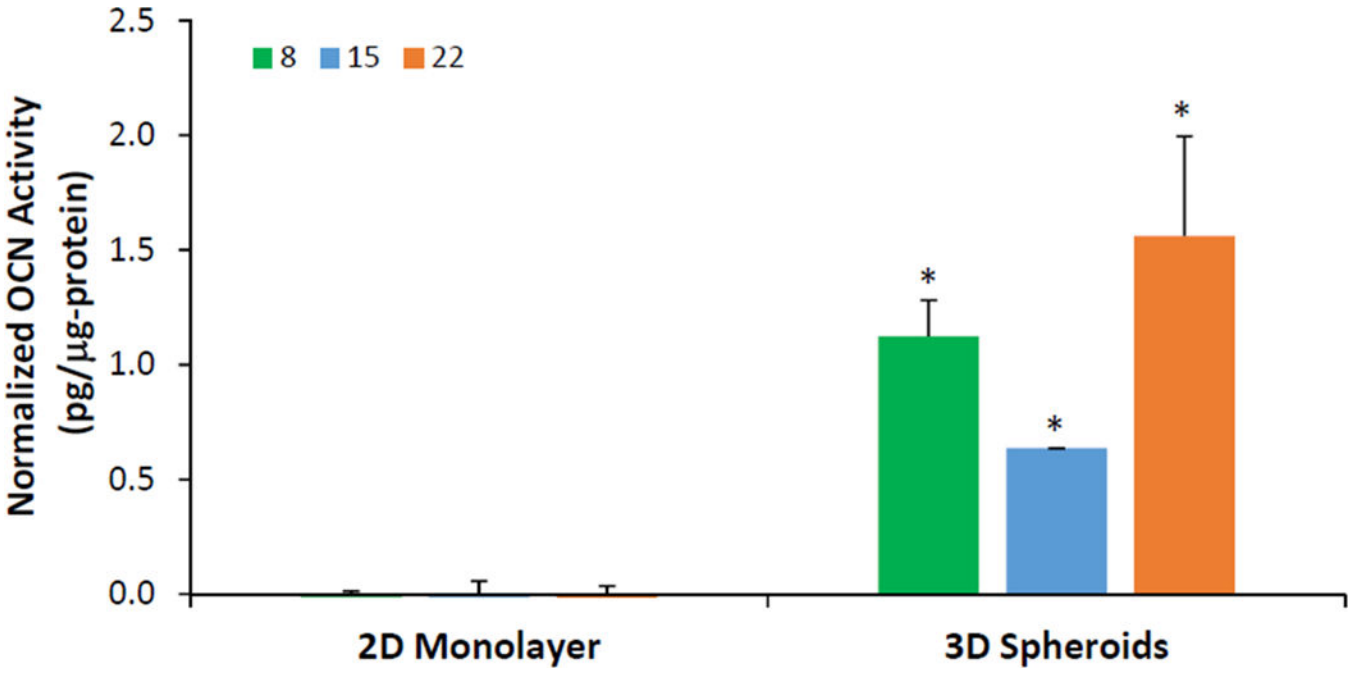

Figure 5.

Osteocalcin content normalized to total protein of hASCs cultured as 2D monolayer and 3D spheroids. Green bars = day 8; blue bars = day 15, orange bars = day 22. Error bars represent 95% confidence intervals. *$p \leq 0.05$ against 2D on the same day.

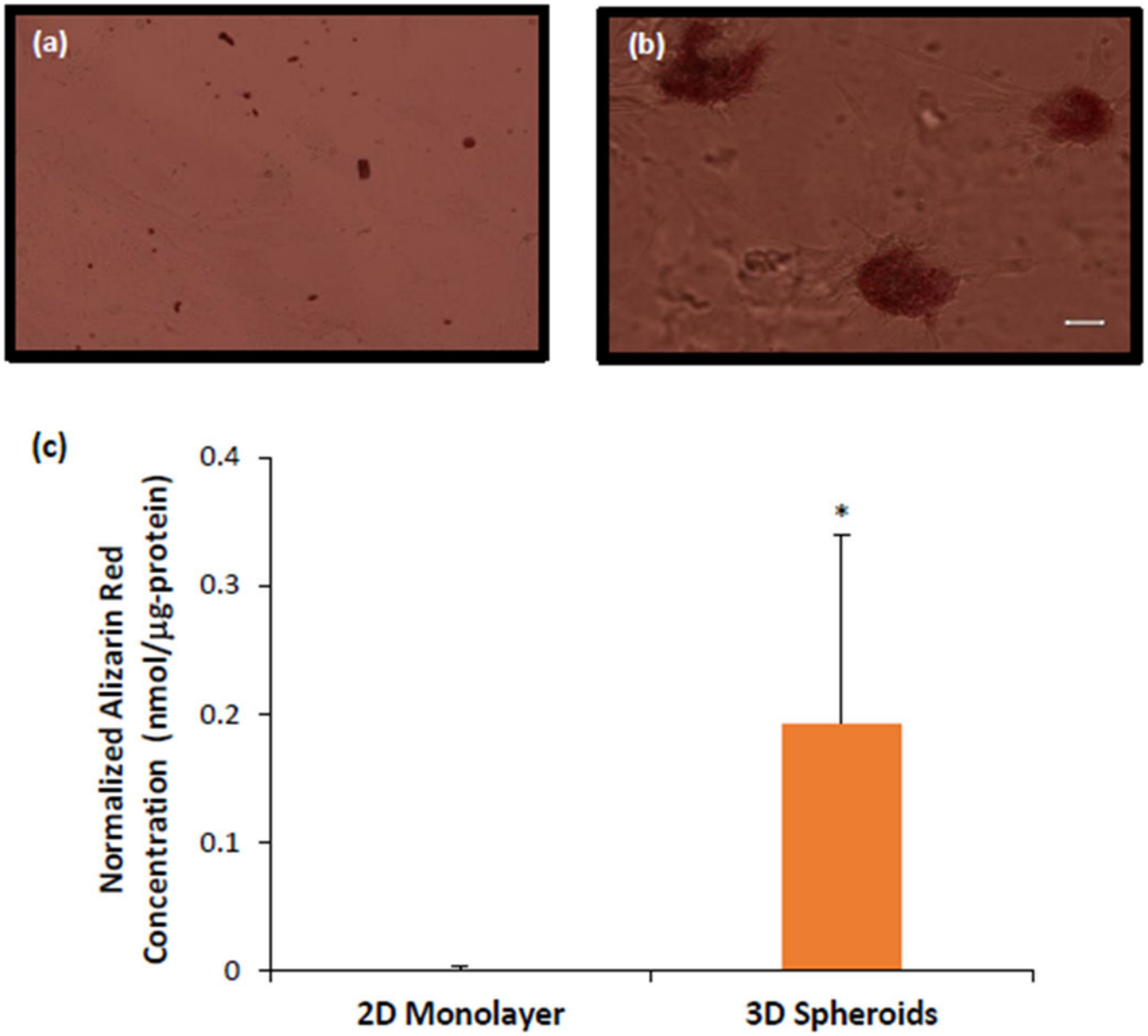

Figure 6.

Alizarin red staining of hASCs cultured as (a) 2D monolayer and (b) 3D spheroids on day 22. (c) Quantification of Alizarin red staining normalized to total protein of hASCs. Scale bar = 50 μm. Error bars represent 95% confidence intervals. *$p \leq 0.05$ against 2D on the same day.